

Sebastian P. Schwaminger<sup>1,2,\*</sup>, Helen Werner,<sup>1</sup> Michael Wengler<sup>1</sup> and Shyam Srinivasan<sup>1</sup>

# Magnetic extraction of calcium oxalate crystals with iron oxide nanoparticles

<https://doi.org/10.1515/cdbme-2022-1156>

**Abstract:** Residual fragments can remain after kidney stone extraction which may necessitate another intervention. Magnetic nanoparticles (MNP) can be applied due to their properties of being able to bind to residual fragments and to be extracted by an external magnetic field. Calcium oxalate crystals and magnetic nanoparticles have been synthesized, characterized and used for binding and magnetic separation studies. The separation is validated by simulation and experimentally. MNP bind covalently to the fractals and a magnetic extraction of calcium oxalate fractals is possible. The agglomeration of MNP can be induced with the addition of salt which improves the extraction process. This proof-of-concept study is the fundament for a new way of stone extraction and can pave the way for new procedures in urology.

**Keywords:** Iron oxide nanoparticles, Magnetic separation, Kidney stones, Agglomeration

## 1 Introduction

Already in ancient Egypt, people suffered from kidney stone disease and the first recorded stone was found in a mummified person who died in 440 BC.[1] To this day, kidney stone disease, urolithiasis, is a widespread disease with increasing prevalence and incidence.[2] There are different types of kidney stones in human bodies which occur depending on the course of disease, medical history, and other patient-specific causes.[3] The most common types are calcium oxalate, calcium phosphate, uric acid, struvite, and cystine stones.[1] All can disturb the urinary drainage system which leads to painful colics and/ or the emergence of more stones.[1] Currently, several therapy forms are applied using a high-power laser system to destroy kidney stones enabling them to pass the urogenital tract.[3, 4] The laser system is often combined with a small basket to grip bigger fragments which

is known as retrograde intrarenal surgery (RIRS).[3] A novel therapy approach employs a frequenting irradiation of holmium or thulium laser to dust or pop-dust the whole stone.[3] The different therapy approaches bear various risks; among others the residue of clinically insignificant fragments (CIRF) with a size < 1 mm.[3] The importance of CIRFs is controversial and new studies suggest that they may be a seed for the formation of new stones requiring additional treatment.[3] Thus, another method to remove the residual fragments is required with the aim to avoid a second treatment. While mechanical extraction using kidney stone retrieval baskets is the most prevalent method, the remaining fragments after the treatment cannot be excluded.[4]

In order to solve this issue of residual fragments, we propose the magnetic extraction. Magnetic extraction originated from magnetic fishing in the mineral industry that has already found its way to food processing, wastewater treatment, and life science applications.[5, 6] Moreover, the magnetic separation of kidney stones has been considered.[7–10] Fernandez et al. simulated the use of a permanent magnet on a ureterorenoscope for the extraction of kidney stones with microscale magnetic beads.[10] Calculations indicate a proof-of-principle for magnetic extraction and Tan et al. used magnetic particles to magnetically extract stones and showed the potential of this technique in comparison to nitinol baskets.[10]

The idea of entire therapy concept is to introduce magnetic particles to the kidney after laser irradiation of kidney stones through an ureterorenoscope and to magnetically extract small kidney stone fractals with a magnetic extraction tool. This is the first study to introduce bare MNP for calcium oxalate crystal extraction. For the development of a clinical extraction method, it is important to define a minimum concentration of MNP required to achieve an adequate removal rate.

## 2 Materials and methods

The MNP were synthesized by co-precipitation as described earlier [11, 12] and stored under nitrogen atmosphere. [13] Calcium oxalate dihydrate crystals were synthesized as described by Werner et al.[14]

The composition of iron oxide nanoparticles and calcium oxalate dihydrate crystals was determined thoroughly with ATR FT-IR, Raman spectroscopy, X-ray diffraction and

\*Corresponding author: Sebastian Schwaminger:

<sup>1</sup>Bioseparation Engineering Group, School of Engineering and Design, Technical University of Munich, Boltzmannstraße 15, 85748 Garching, Germany, e-mail: s.schwaminger@tum.de

<sup>2</sup>Otto Loewi Research Center, Division of Physiological Chemistry, Medical University of Graz, Neue Stiftingtalstraße 6, 8010 Graz, Austria, e-mail: sebastian.schwaminger@medunigraz.at

microscopy.[13, 14] Dynamic light scattering and zeta potential measurements were conducted with a Delsa Nano C (Beckman Coulter Inc., USA) in order to determine hydrodynamic diameter and the zeta potential. The analysis in a centrifugal field was performed with a LUMiSizer (LUM GmbH, Germany) with 200 profiles in an interval of 5 s with 400 g and a light factor of 0.25. For the sedimentation analysis and the magnetic sedimentation experiments a LUMiReader (LUM GmbH, Germany) with a cuvette holder containing either a permanent magnet (400 mT at surface) or a reference. Cuvettes (10 mm x 10 mm x 45 mm) were filled with 3 mL. The absorbance measurements with 870 nm, 630 nm and 410 nm lasers were conducted at 6, 10.5 and 16 mm distance to the magnet, respectively. A profile was measured every second and 200 profiles were considered for the determination of the sedimentation velocity. Magnetic flux and gradient of the field amounted to 66 mT, and 0.14 T m<sup>-1</sup>, respectively. Microscopic images were made with an AXIO Observer from Zeiss with the Axiocam 506 mono. Pictures were generated with a fluorescent lamp in bright-field with 12% intensity for 500 ms.

The magnetic nanoparticle concentration was adjusted to 1 g L<sup>-1</sup> for all samples while the calcium oxalate concentration varied between 0.1 and 1 g L<sup>-1</sup>. The pH value was adjusted to 5 with hydrochloric acid in both solutions before mixing.

For the binding kinetics, 2 mL of the mixtures (1:1) were shaken at 300 rpm and were incubated for different times (30, 60, 120, 300 s) at 37 °C. Afterwards, the samples were put in an external magnetic field, after 30 s the supernatant was filled in a 96-well plate and measured at 600 nm with a microplate reader Infinite M200 from Tecan. The samples were measured two times and the experiments were repeated three times.

The MNP concentration was adjusted to 1 g L<sup>-1</sup> and the calcium oxalate concentration to 1 g L<sup>-1</sup>. The salt concentration varied between 10 and 100 mmol L<sup>-1</sup>. The experiments were conducted similarly to the kinetics and incubated for 120 s. The samples were measured twice and the experiments were repeated three times.

The removal was performed in an external magnetic field generated by a hand magnet (Block magnet 40 mm x 40 mm x 20 mm, Neodymium, N42, nickel-plated, Webcraft GmbH, Germany). It was positioned at distances of 0, 0.5, 1.0, 2.5, 5.0 cm. The removal rate equals the difference of initial and the supernatant concentration of oxalate. The magnetic flux was determined at the same distances with a Gaussmeter (PCE-MFM 3000). The magnetic flux was measured three times, the samples two times and the whole experiment was repeated three times. LUMiReader was used to measure the particle velocity. The samples were prepared with a MNP and calcium oxalate concentration of 1 g L<sup>-1</sup> in a cuvette. The pH was adjusted to 5 in all solutions before mixing. The total volume

was 2 mL and each sample was filled up with deionized water at 2 mL. The calcium oxalate solution was added last and after 60 seconds the samples were resuspended and measured with 300 profiles in 0.5 seconds with a light factor of 1.

COMSOL Multiphysics® was used for simulation studies. The magnetic properties for iron oxide nanoparticles were derived from the magnetometry studies of Thomas et al. (permeability of MNP = 9). [13] The density of the materials were set to 5.2 g cm<sup>-3</sup> for iron oxides and to 2.12 g cm<sup>-3</sup> for calcium oxalate fractals. The velocity equals the sum of magnetophoretic velocity, the gravitational velocity and Stokes' drag. The removal rate is equals the quotient of magnetophoretic force and gravitational force on the particles. The gravitational force is dependent on the density difference between particles and fluid  $\rho_p - \rho_f$  (1.87 g cm<sup>-3</sup>),  $g$  (9.81 m s<sup>-2</sup>) and the particle radius  $r$  as given in Eq. 1:

$$F_g = (\rho_p - \rho_f)g \frac{4}{3}\pi r^3 \quad (1)$$

The magnetophoretic force describes the resultant force acting on the particle due to an external magnetic field and is dependent on the particle radius  $r$ , the permeabilities ( $\mu_0 = 1.25664 \cdot 10^{-6}$ ,  $\mu_r = 1$ ,  $\mu_{r,p} = 9$ ) the relative permeability  $K = \frac{\mu_{r,p} - \mu_r}{\mu_{r,p} + 2\mu_r}$  and the magnetic field gradient  $\nabla H$ :

$$F_m = 3\mu_0\mu_r K \nabla H^2 \pi r^3 \quad (2)$$

The velocity is further dependent on viscosity  $\mu$ :

$$v = \frac{2(\rho_p - \rho_f)gr^2}{9\mu} + \frac{\mu_0\mu_r K \nabla H^2 r^2}{2\mu} \quad (3)$$

The buoyancy and the friction force are overcome by the magnetophoretic force (magnetophoresis).[15, 16]

## Results and discussion

Magnetic nanoparticles (MNP) were synthesized by a simple low-cost co-precipitation method as described by Roth et al.[12, 13] The physical properties such as saturation magnetization (84 Am kg<sup>-1</sup>), no remanence, an isoelectric point around pH 6, the chemical composition Fe<sub>3</sub>O<sub>4</sub> and the crystalline spinel structure were previously described by Thomas et al.[13]. Nanoparticles demonstrate a sharp size distribution with a mean diameter of 10 nm, a specific surface area of around 89 m<sup>2</sup> g<sup>-1</sup>. [13] The high magnetizations (56 Am kg<sup>-1</sup> and 47 Am kg<sup>-1</sup>) at low magnetic fields of 200 mT and 100 mT, respectively, enables the use of these particles for magnetic separation applications.[6, 17] The ionic strength affects the agglomeration behavior of MNP: Hydrodynamic diameters increase significantly from 140 nm to 2780 nm and 1420 nm for 0, 0.1 and 1 M NaCl, respectively (Fig. 1a). In

magnetic sedimentation experiments with an average magnetic field of 66 mT, the trend to higher sedimentation velocities with higher concentration of sodium chloride is evident (Fig. 1b). The median sedimentation velocity of MNP in deionized water amounts to  $140 \mu\text{m s}^{-1}$ . The addition of salt leads to a significantly increased median sedimentation velocity of  $1110 \mu\text{m s}^{-1}$  and  $3110 \mu\text{m s}^{-1}$  for 0.1 M and 1 M salt, respectively. This significant increase of velocity can be explained by increasing particle sizes of agglomerates which not only lead to an increased gravitational but also increased magnetophoretic sedimentation velocity (Eq. 3).

We want to emphasize the use of very small fractals which might otherwise not be extracted in kidneys (CIRFs).

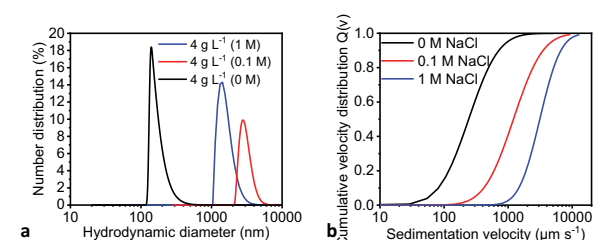


**Figure 1:** a Hydrodynamic diameters of  $4 \text{ g L}^{-1}$  MNP with 0 M, 0.1 M and 1 M NaCl determined by DLS. b Cumulative sedimentation velocity distributions.

CIRFs can be very heterogeneous in size but usually have the same phase and physical properties.[14] Thus, we used synthesized calcium oxalate crystals.[14]

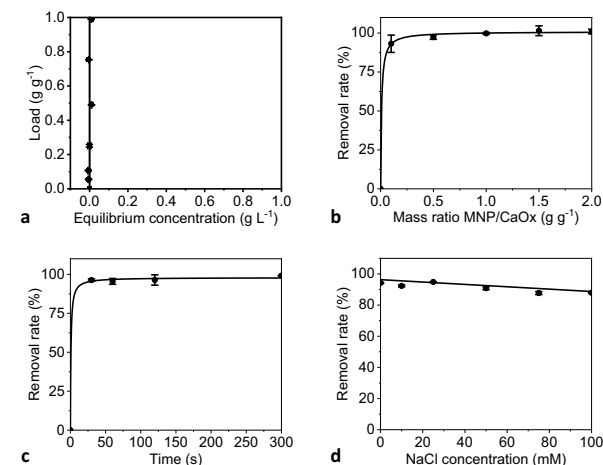


**Figure 2:** a Load of calcium oxalate dihydrate (CaOx) on MNP. b Removal rate (mass ratio) c Removal rate (incubation time) d Removal rate (salt concentration)

Binding studies of MNPs and calcium oxalate crystals were conducted at  $37 \text{ }^\circ\text{C}$  to emulate the temperature in a human kidney. Therefore, similar to a classical adsorption isotherm, calcium oxalate concentration was varied ( $0.1 - 1 \text{ g L}^{-1}$ ) while the MNP concentration was kept constant ( $1 \text{ g L}^{-1}$ ). However, in Fig. 2a we do not observe a classical adsorption behavior with increasing loads for higher equilibrium concentrations. In all experiments, calcium oxalate directly adsorbs to iron oxide nanoparticles and therefore no

supernatant concentration can be observed. This strongly indicates an irreversible binding behavior for calcium oxalate and MNPs. With this experimental evidence for the complexation of MNPs with oxalate, which is well-known,[18] we investigated the MNP concentration to remove fractals of a defined concentration. Figure 2b indicates a high removal rate of calcium oxalate fractals ( $>95 \%$ ) even for a MNP to calcium oxalate ratio of 0.25. The removal rate demonstrates a sigmoidal increase with increasing MNP to calcium oxalate ratio and a rate of  $>99 \%$  is reached at a ratio of 1 and stayed constant for higher ratios. The removal rate has been investigated as a function of the incubation time (Fig. 2c). The graph shows a sigmoidal increase with reaction time and reaches a maximum at two minutes. This indicates a fast

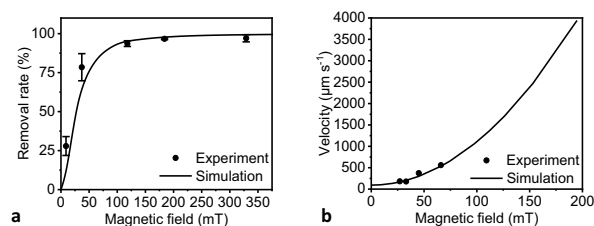


**Figure 3:** a Removal rate depending on the magnetic field. b Particle velocity depending on the magnetic field.

binding kinetic between the two components. As shown in Fig. 1, the addition of sodium chloride improves the magnetic separation efficiency of MNP. The ionic strength directly affects the electrostatic repulsion between two similar particles, which can be observed from zeta potential. While the aggregation of similarly charged particles can be beneficial for the process, the same effect leads to a reduced electrostatic attraction between oppositely charged species such as MNP and oxalate fractals. However, the results shown in Fig. 1d verify the assumption of an irreversible bond formation between MNP and oxalate. The removal rate is slowly decreasing with increasing salt concentration, but also at high salt concentrations a removal rate of over 90% can be reached. Chloride ions can affect the zeta potential of the nanoparticles and thus the electrostatic repulsion potential.[18] The required magnetic field strength was evaluated by investigating the removal rate and the particle velocity in dependence of the magnetic field. Fig 3a shows an sigmoidal increase of the removal rate with increasing magnetic field. That means with an increasing magnetic field more calcium oxalate fragments can be removed by magnetic nanoparticles. It is possible to remove 97 % of the calcium oxalate fragments with a magnetic field of 184 mT. The magnetophoretic force must be higher than the buoyancy and the gravitational force to enable magnetophoresis.[19] The size of the agglomerates is the decisive property which determines the particle velocity.[16] For our simulation, we assumed a particle diameter of  $9 \mu\text{m}$  and an average of density and permeability of MNPs and

calcium oxalate. The model and the obtained velocities are in good agreement with the settling behavior of magnetic beads in magnetic fields.[20] Further effects such as magnetic convection and magnet-induced aggregation, which very likely occur, are not considered in this model.[21]

### 3 Conclusion

This study shows that calcium oxalate crystals can be magnetically separated with MNPs in even small magnetic fields below 100 mT. MNPs irreversibly bind to calcium oxalate and form magnetic agglomerates. These agglomerates can be manipulated magnetophoretically in magnetic fields and behave similar to the simulation. These findings and the high biocompatibility [5, 6] imply the possibility of using MNPs for kidney stone extraction. We hope that our investigation will pave the way for simpler approaches towards residue free kidney stone removal.

#### Author Statement

We appreciate the support of: BMBF and ESF (EXIST), the StMWi (FLÜGGE), DFG and TUM in the framework of the OAPP. SPS, MW and SS filed a patent application on the use of iron oxide nanoparticles for the extraction of kidney stones. Informed consent has been obtained from all individuals included in this study. The conducted research is not related to human or animals use. We thank Michael Schobesberger for help with light microscopy, Leonie Wittmann for help with COMSOL, Dr. Madleen Busse and Prof. Sonja Berensmeier for fruitful discussions. The datasets of this study are available from the corresponding author on reasonable request.

### References

- [1] Stoller ML, Meng MV (2007) Urinary Stone Disease: The Practical Guide to Medical and Surgical Management. Curr Clin Urol. Humana Press Inc, Totowa, NJ
- [2] Romero V, Akpınar H, Assimos DG (2010) Kidney stones: a global picture of prevalence, incidence, and associated risk factors. Rev Urol 12:e86-96
- [3] Weiss B, Shah O (2016) Evaluation of dusting versus basketing - can new technologies improve stone-free rates? Nat Rev Urol 13:726–733
- [4] Pietropaolo A, Reeves T, Aboumarzouk O et al. (2020) Endourologic Management (PCNL, URS, SWL) of Stones in Solitary Kidney: A Systematic Review from European Association of Urologists Young Academic Urologists and Uro-Technology Groups. J Endourol 34:7–17
- [5] Katz E (2020) Magnetic Nanoparticles. Magnetochemistry 6:6
- [6] Schwaminger SP, Fraga-García P, Eigenfeld M et al. (2019) Magnetic Separation in Bioprocessing Beyond the Analytical Scale: From Biotechnology to the Food Industry. Front Biotechnol Bioeng 7:233
- [7] Tan YK, Best SL, Donnelly C et al. (2012) Novel iron oxide microparticles used to render stone fragments paramagnetic: assessment of toxicity in a murine model. J Urol 188:1972–1977
- [8] Tan YK, McLeroy SL, Faddegon S et al. (2012) In vitro comparison of prototype magnetic tool with conventional nitinol basket for ureteroscopic retrieval of stone fragments rendered paramagnetic with iron oxide microparticles. J Urol 188:648–652
- [9] Tracy CR, McLeroy SL, Best SL et al. (2010) Rendering stone fragments paramagnetic with iron-oxide microparticles improves the efficiency and effectiveness of endoscopic stone fragment retrieval. Urology 76:1266.e10-4
- [10] Fernandez R, Tan YK, Kaberle W et al. (2012) Determining a performance envelope for capture of kidney stones functionalized with superparamagnetic microparticles. J Endourol 26:1227–1230
- [11] Schwaminger SP, Syhr C, Berensmeier S (2020) Controlled Synthesis of Magnetic Iron Oxide Nanoparticles: Magnetite or Maghemite? Crystals 10:214
- [12] Roth H-C, Schwaminger SP, Schindler M et al. (2015) Influencing factors in the Co-precipitation process of superparamagnetic iron oxide nano particles: A model based study. J Magn Magn Mater 377:81–89
- [13] Thomas JA, Schnell F, Kaveh-Baghbaderani Y et al. (2020) Immunomagnetic Separation of Microorganisms with Iron Oxide Nanoparticles. Chemosensors 8:17
- [14] Werner H, Bapat S, Schobesberger M et al. (2021) Calcium Oxalate Crystallization: Influence of pH, Energy Input, and Supersaturation Ratio on the Synthesis of Artificial Kidney Stones. ACS Omega 6:26566–26574
- [15] Alnaimat F, Mathew B (2020) Magnetophoretic microdevice for size-based separation: model-based study. Eng Appl Comput Fluid Mech 14:738–750
- [16] Yan H, Wu H (2008) Magnetophoresis. In: Li D (ed) Encyclopedia of Microfluidics and Nanofluidics. Springer US, Boston, MA, pp 1043–1048
- [17] Franzreb M, Siemann-Herzberg M, Holey TJ et al. (2006) Protein purification using magnetic adsorbent particles. Appl Microbiol Biotechnol 70:505–516
- [18] Schwaminger SP, Schwarzenberger K, Gatzemeier J et al. (2021) Magnetically Induced Aggregation of Iron Oxide Nanoparticles for Carrier Flotation Strategies. ACS Appl Mater interfaces 13:20830–20844
- [19] Lin S, Lu D, Liu Z (2012) Removal of arsenic contaminants with magnetic  $\gamma$ -Fe<sub>2</sub>O<sub>3</sub> nanoparticles. Chem Eng J 211-212:46–52
- [20] Ng WM, Katiyar A, Mathivanan V et al. (2020) Sedimentation Kinetics of Magnetic Nanoparticle Clusters: Iron Oxide Nanospheres vs Nanorods. Langmuir 36:5085–5095
- [21] Leong SS, Ahmad Z, Low SC et al. (2020) Unified View of Magnetic Nanoparticle Separation under Magnetophoresis. Langmuir 36:8033–8055